The Astronomical Journal, 131:49–54, 2006 January

A SNAPSHOT SURVEY FOR GRAVITATIONAL LENSES AMONG $z \geq 4.0$ QUASARS. II. CONSTRAINTS ON THE $4.0 < z < 5.4$ QUASAR POPULATION[1]

Gordon T. Richards,[2] Zoltán Haiman,[3] Bartosz Pindor,[4] Michael A. Strauss,[2] Xiaohui Fan,[5] Daniel Eisenstein,[5] Donald P. Schneider,[6] Neta A. Bahcall,[2] J. Brinkmann,[7] and Masataka Fukugita[8]

Received 2005 July 7; accepted 2005 September 5

ABSTRACT

We report on *i*-band snapshot observations of 157 Sloan Digital Sky Survey quasars at $4.0 < z < 5.4$ using the Advanced Camera for Surveys on the *Hubble Space Telescope* (*HST*) to search for evidence of gravitational lensing of these sources. None of the quasars appear to be strongly lensed and multiply imaged at the angular resolution ($\sim 0\farcs1$) and sensitivity of *HST*. The nondetection of strong lensing in these systems constrains the $z = 4-5$ luminosity function to an intrinsic slope of $\beta > -3.8$ ($3\,\sigma$), assuming a break in the quasar luminosity function at $M^*_{1450} \sim -24.5$. This constraint is considerably stronger than the limit of $\beta > -4.63$ obtained from the absence of lensing in four $z > 5.7$ quasars. Such constraints are important to our understanding of the true space density of high-redshift quasars and the ionization state of the early universe.

Key words: early universe — galaxies: luminosity function, mass function — gravitational lensing — quasars: general

Online material: machine-readable tables

1. INTRODUCTION

Investigations of multiply imaged high-redshift quasars are important to our basic understanding of the formation and growth of supermassive black holes in galactic centers (Turner 1991; Haiman & Loeb 2001) and the ionization state of the universe as a function of time (Madau et al. 1999; Wyithe & Loeb 2003a). Gravitational lensing changes the apparent flux coming from a quasar and thus changes our interpretation of flux-dependent properties; the discovery that a given quasar is gravitationally lensed means that the naively estimated luminosity is too high. Thus, gravitational lensing would modify the expected size of ionized (H II) regions around individual quasars (Cen & Haiman 2000) and weaken the lower limits on the neutral fraction in the intergalactic medium as inferred from the sizes of H II regions (Wyithe & Loeb 2004; Mesinger & Haiman 2004). This paper concentrates on the effect that gravitational lensing has on the apparent shape of the quasar luminosity function (QLF; Comerford et al. 2002; Wyithe & Loeb 2002; Fan et al. 2003). In a previous paper (Richards et al. 2004, hereafter Paper I) we investigated whether the known $z \sim 6$ quasars are gravitationally lensed and discussed how the lack of lenses in this sample affects our understanding of the growth of black holes in the early universe (e.g., Haiman & Loeb 2001) and the ionization history of the universe at the end of the reionization period (e.g., Fan et al. 2002). In this paper we examine the constraints that can be placed on the intrinsic slope of the QLF at $z \sim 4-5$ from a search for gravitational lenses in a sample of $z \sim 4-5$ quasars (Fan et al. 2001a; Anderson et al. 2001; Schneider et al. 2001, 2005) in the Sloan Digital Sky Survey (SDSS; York et al. 2000).

Much theoretical effort has been devoted to placing constraints on the slope of the QLF from the fraction of lenses found among high-z quasars (e.g., Comerford et al. 2002; Wyithe & Loeb 2002). Comerford et al. (2002) showed that modest constraints could be obtained from a sample of ~ 20 $z \sim 6$ quasars from ground-based imaging (i.e., sensitive to $\geq 1''$ splittings) and that similar limits could be derived from *Hubble Space Telescope* (*HST*) resolution imaging of the (then) four known $z \sim 6$ quasars. Paper I presented *HST* imaging showing that none of those four quasars are strongly gravitationally lensed and derived a limit on the slope of the bright-end QLF of $\beta > -4.63$ ($3\,\sigma$). Wyithe (2004) found even stronger constraints for this sample by including the observation that two quasars appear to be lensed by foreground galaxies but are not multiply imaged.

These limits come from magnification bias (Turner et al. 1984; Narayan 1989), which would be strong if the slope of the QLF were steep and there were many quasars with intrinsic luminosities below the detection threshold. As discussed in Paper I, the expected fraction of multiply imaged quasars at a given redshift depends both on the cosmological model and on the QLF. In the *Wilkinson Microwave Anisotropy Probe* (*WMAP*) cosmology (Spergel et al. [2003], using a halo distribution taken from the large N-body simulations of Jenkins et al. [2001]), the fraction of random lines of sight out to $z = 4$ that produce multiple images at all splitting angles is on the order of 0.2%; this fraction rises to $\sim 0.4\%$ at $z = 6$. If the intrinsic (unlensed) QLF has a break in slope, then, in general, the fraction of lensed quasars would increase for apparent fluxes above the break. In a flux-limited survey, there is a strong correlation between luminosity and redshift. If the true QLF possesses a break that moves to fainter luminosities at higher redshift, then the most distant quasars (which

[1] Based on observations made with the NASA/ESA *Hubble Space Telescope*, obtained at the Space Telescope Science Institute, which is operated by the Association of Universities for Research in Astronomy, Inc., under NASA contract NAS5-26555. These observations are associated with program 9472.

[2] Princeton University Observatory, Peyton Hall, Princeton, NJ 08544.
[3] Department of Astronomy, Columbia University, 550 West 120th Street, New York, NY 10027.
[4] Department of Astronomy, University of Toronto, 60 St. George Street, Toronto, ON M5S 3H8, Canada.
[5] Steward Observatory, University of Arizona, 933 North Cherry Avenue, Tucson, AZ 85721.
[6] Department of Astronomy and Astrophysics, Pennsylvania State University, 525 Davey Laboratory, University Park, PA 16802.
[7] Apache Point Observatory, P.O. Box 59, Sunspot, NM 88349.
[8] Institute for Cosmic Ray Research, University of Tokyo, 5-1-5 Kashiwa, Kashiwa City, Chiba 277-8582, Japan.

TABLE 1

SDSS J (1)	Redshift (2)	M_B (3)	SDSS i (4)	*HST* i (5)	$P_{\rm lens,0}$ (6)	$P_{\rm lens}$ (7)	*HST* ID (8)	Ref. (9)
001115.23+144601.8.....	4.924	−29.48	18.41	18.26	0.3137	0.0906	aa	7
001134.52+155137.3	4.394	−27.23	20.20	19.91	0.0553	0.0164	ab	7
001714.66−100055.4	4.976	−27.94	19.61	19.46	0.1103	0.0277	ac	7
001813.88+142455.6	4.221	−27.83	19.41	19.30	0.0945	0.0269	ad	7
001918.43+150611.3	4.134	−27.27	19.91	19.94	0.0563	0.0160	ae	7

NOTES.—Table 1 is published in its entirety in the electronic edition of the *Astronomical Journal*. A portion is shown here for guidance regarding its form and content. Col. (1): IAU name of the object (note that SDSS image reprocessing can change the coordinates [by ∼0.″1] and thus the name slightly; matching should thus be done on coordinates, not names). Starred objects were selected without reference to their morphological type (stellar vs. extended). Col. (2): Redshift. Col. (3): Absolute B magnitude, computed with the parameters given in § 1. Cols. (4) and (5): SDSS and *HST* i-band magnitudes (uncorrected for Galactic reddening). Col. (6): Lensing probability for this object, ignoring morphological selection effects. Col. (7): Lensing probability after accounting for morphological selection effects. Col. (8): Two character "observation set ID" related to the *HST* file-naming convention. This is given to facilitate archival use of these data. The program ID for this project was "8f3," and thus, the files for the first object have names in the form j8f3aa011_crj.fits.

REFERENCES.—(1) Fan et al. 1999; (2) Fan et al. 2000; (3) Fan et al. 2001a; (4) Zheng et al. 2000; (5) Schneider et al. 2001; (6) Anderson et al. 2001; (7) Schneider et al. 2005. A zero in this column means that the objects are being published here for the first time.

also look through the longest path length) are expected to be the most likely to be lensed. More explicitly, in the event that no lensing is observed Paper I showed that the tightest constraints on the QLF slope come from $z \sim 6$ quasars and also that roughly seven $z \sim 4$ quasars have the same statistical power as a single $z \sim 6$ quasar. Herein we present the results for a sample of 157 $z \sim 4$ quasars from the SDSS that were imaged with *HST*; we find that none of these sources is lensed. As predicted, these quasars provide a constraint on the slope of the QLF that is roughly equivalent to *HST* imaging of 22 $z \sim 6$ quasars, limiting the bright-end slope of the $z = 4$–5 QLF to $\beta > -3.8$ (3 σ).

Section 2 describes the sample and the data. In § 3 we discuss the constraints on the QLF that can be derived from the data. We summarize in § 4. Throughout this paper we adopt the *WMAP* cosmology with $\Omega_m = 0.3, \Omega_\Lambda = 0.7, H_0 = 70$ km s^{-1} Mpc^{-1}, an rms mass fluctuation within a sphere of radius 8 h^{-1} Mpc of $\sigma_8 = 0.9$, and a power-law index $n = 0.99$ for the power spectrum of density fluctuations (Spergel et al. 2003). We also adopt the cosmological transfer function from Eisenstein & Hu (1999). Conversions between M_B and M_{1450} assume $M_B = M_{1450} - 0.48$ (Schmidt et al. 1995) with spectral index $\alpha_\nu = -0.5$ ($f_\nu \propto \nu^{\alpha_\nu}$).

2. THE DATA

2.1. *Observations and Data Processing*

There were 281 SDSS quasars with $z \geq 4.0$ as of 2002 January (Fan et al. 1999, 2000, 2001a; Zheng et al. 2000; Schneider et al. 2001; Anderson et al. 2001), when the sample was defined. Most of these were included in the SDSS spectroscopy, but several were discovered as part of early follow-up spectroscopy on the Astrophysical Research Consortium (ARC) 3.5 m telescope and other telescopes (e.g., Fan et al. 1999), including some that have not yet been published. We were granted the opportunity to observe 250 of these in *HST* snapshot mode; we did so by including in the sample all quasars with $z \geq 4.6$ and all quasars with $4.0 < z < 4.6$ with $i < 20.3$.

Snapshot observations are carried out with the understanding that not all objects will be observed. In this context, we were able to give objects priorities for being observed. We put the 48 objects with an absolute 1450 Å magnitude less than −29 and/or with $z > 5$ at highest priority and those with $M_{1450} > -27.95$ at lowest priority. All remaining objects, and those with $4.7 < z < 5$, were placed at medium priority. At the end, 161 objects were observed (of which four were presented in Paper I): 48/48 of the high-priority objects, 97/154 of the medium-priority objects, and 16/48 of the low-priority objects.

The four $z > 5.7$ quasars included in our *HST* snapshot program were presented in Paper I. In this paper we describe the results of imaging 157 SDSS quasars with $4 < z < 5.4$ (see Table 1). For the sake of completeness, we also tabulate those 89 sources that were included in our sample but were never observed by *HST* (see Table 2). Seven objects in Table 1 and five objects in Table 2 are previously unpublished.

Images of the 157 quasars were acquired with the High Resolution Camera (HRC) on the Advanced Camera for Surveys (ACS). Observations were taken in the SDSS i-band (F775W). The Wide-Field Camera on ACS has higher sensitivity in i than does the HRC but has substantially higher overhead and is mildly undersampled. The exposure times were 640 s for each object: 320 s in each of two exposures to help in cosmic-ray rejection.

The data processing was discussed in detail in Paper I, but we briefly review the process here. The raw images were calibrated by the CALACS package in IRAF[9] as part of on-the-fly

[9] IRAF is distributed by the National Optical Astronomy Observatory, which is operated by the Association of Universities for Research in Astronomy, Inc., under cooperative agreement with the National Science Foundation.

TABLE 2

SDSS J (1)	Redshift (2)	SDSS i (3)	Ref. (4)
003126.80+150739.6	4.291	19.97	7
010326.89+005538.6	4.159	20.07	0
015032.87+143425.5	4.284	20.09	6
020152.53−094733.4	4.026	20.29	7
021419.42−010716.9	4.592	20.53	0

NOTES.—Table 2 is published in its entirety in the electronic edition of the *Astronomical Journal*. A portion is shown here for guidance regarding its form and content. Col. (1): IAU name of the object (note that SDSS image reprocessing can change the coordinates [by ∼0.″1] and thus the name slightly; matching should thus be done on coordinates, not names). Starred objects were selected without reference to their morphological type (stellar vs. extended). Col. (2): Redshift. Col. (3): SDSS i-band magnitude (uncorrected for Galactic reddening).

REFERENCES.—(1) Fan et al. 1999; (2) Fan et al. 2000; (3) Fan et al. 2001a; (4) Zheng et al. 2000; (5) Schneider et al. 2001; (6) Anderson et al. 2001; (7) Schneider et al. 2005. A zero in this column means that the objects are being published here for the first time.

reprocessing (OTFR) at the time of download. The images that we present are the "cosmic-ray-rejected" (CRJ) images that are output by the OTFR algorithms at the Space Telescope Science Institute. The CRJ files have all been reduced in the standard manner, including having been overscan-, bias-, and dark-corrected, flat-fielded, and photometrically calibrated, in addition to having bad pixels masked and cosmic rays removed (see the ACS manual[10] for more details).

2.2. *Subtracting the Point Source and Looking for Multiple Images*

HST-resolution data are needed for this project, as the median expected splitting of gravitationally lensed quasars is predicted (and observed) to be somewhat less than 1″ (Turner et al. 1984; Hinshaw & Krauss 1987; Browne et al. 2003), and the SDSS images themselves have point-spread function (PSF) widths of order 1″–1.″8 (Abazajian et al. 2003) with an image scale of 0.″396 pixel^{-1}. Our ACS images, on the other hand, have an image scale of 0.″025 pixel^{-1}, and the PSF is narrow enough that any lens with a separation greater than $\sim$0.″2 will be obvious by visual inspection, as we show explicitly in Paper I. These observations should therefore be sensitive to essentially all expected lenses.

We search for faint secondary images at separations smaller than a few tenths of an arcsecond by fitting and removing a model for the PSF of each image. We use version 6.1 (which includes on-orbit updates for ACS) of the Tiny Tim software (Krist 1995),[11] which produces a model PSF for the instruments on *HST* given the object's (observed) spectral energy distribution and position in the focal plane, the filter curve, and knowledge of the optics of the instrument. We fit the PSF model to each CRJ image, allowing the location on the CCD and normalization to vary and using sinc interpolation when shifting the model PSF by fractional pixels. Example PSF-subtracted images are shown in Figure 1. Each of the images shows the familiar first Airy ring; on a very hard stretch, the second Airy ring is faintly visible.

As discussed in Paper I, for a secondary image offset by 0.″1 with a flux ratio of 10:1 the secondary object is visible as an enhancement in the first Airy ring of the primary object; it becomes clear on PSF subtraction (Fig. 1). With a flux ratio of 100:1 we cannot discern a pair with 0.″1 separation even after subtraction of the PSF; however, even if we were able to do so it would not significantly improve the constraints that we derive below, since most split images will have larger image separations.

None of our 157 targets appear to be gravitationally lensed. Figure 1 shows only the 10 objects (both with and without PSF subtraction) that displayed any hint of a second object within the 5″ field of view. Based on their brightness and morphology, these secondary objects are most likely to be galaxies along the line of sight to the target objects or (in some cases) uncorrected cosmetic defects.

2.3. *Accounting for Extended-Source Selection Effects*

Since a gravitationally lensed pair of quasars with a separation roughly comparable to the seeing size may be classified as extended (rather than point) sources, we must account for the effect that a morphological selection criterion has on our analysis. For the very highest redshift ($z \gtrsim 5$) quasars found from SDSS imaging (e.g., Fan et al. 2001a and references therein), there is no selection bias against lensed quasars, since no morphology restriction was imposed. However, for somewhat lower redshift sources, which were selected with the automated pipeline (Richards et al. 2002), there is a strong bias against high-z ($z \gtrsim 3$) quasars that appear extended (whether due to lensing or errors in morphological classification as a result of low signal-to-noise ratio [S/N]). This bias is intentional; the survey cannot afford the fibers that would be needed to explore all the extended sources in the high-z quasar portion of the SDSS color-color diagram. The vast majority of these objects are faint moderate-redshift ($0.4 < z < 1$) galaxies.

As discussed in Paper I and Pindor et al. (2003), in order to test the ability of the SDSS photometric pipeline to identify quasar pairs we created simulated SDSS images of pairs of point sources in these observing conditions and at the appropriate S/N. The SDSS star-galaxy separator would have classified as a galaxy, and hence excluded from the spectroscopic sample, any pair of point sources having both an image separation $\sim 1'' < \Delta\theta <\sim 2''$ and a flux ratio less than $\sim 5:1$. Thus, the SDSS data are suitable for exploring only a fraction of the parameter space of lensing (in terms of separations and flux ratios) that is of interest.

The morphological selection likelihood depends on the luminosity and on the assumed lensing flux ratio and splitting angle for any given individual quasar. We therefore fold this bias into our probability calculations below on an object-by-object basis. For a given quasar in our sample that has an apparent magnitude of i_s at redshift z_s and for a given hypothesized magnification factor μ_s [which for a singular isothermal sphere (SIS) implies a flux ratio of $(\mu_s + 2)/(\mu_s - 2)$] for a lensing halo of mass M (which determines the splitting angle θ_s), we compute the probability $P_s(i_s, z_s, \mu_s, M)$ that the object would have been classified as extended and discarded by the photometric pipeline.

To compute the impact of the selection on our final constraints, we compute the product of the selection likelihood and the expected lensing probability, which gives the probability that this quasar would have been selected by SDSS *and* strongly lensed:

$$P_{\rm lens}(z,\ M) = [1 - P_s(i_s,\ z_s,\ \mu_s,\ M)]\, P_{\rm lens,0}(\mu_s,\ M),$$

where $P_{\rm lens,0}$ is the probability of multiply-imaged lensing in the absence of any other selection effects. Finally, we integrate this product over all combinations of magnifications and lensing halo masses that yield two detectable images with *HST*. We find that typically the inclusion of the morphological selection reduces the total lensing probability by a factor of 3 [i.e., the value of the above-defined integral would be 3 times larger if the factor $P_s(i_s, z_s, \mu_s, M)$ were excluded]. More specifically, we find that only approximately one-third of true lenses would have made it into our sample, with approximately two-thirds being classified as extended sources. In Table 1 we list the overall lensing probability for each source. Sixteen of the 157 sources were selected without regard to morphology (as indicated in Table 1); we therefore did not apply the selection function to these objects.

We note that there is a further possible selection effect due to the fact that PSF magnitudes do not contain 100% of the flux from a gravitationally lensed pair of images, hence effectively reducing the magnification bias. This effect turns out to be less significant, partly because those lensed objects for which it would be most important are already removed from the sample by the star-galaxy morphological bias. Overall, we find that the effect is likely to shift the luminosity scale by $\sim$0.1 mag or less, and we ignore it in what follows.

[10] See http://www.stsci.edu/hst/acs/documents/handbooks/cycle12/cover.html.
[11] See http://www.stsci.edu/software/tinytim.

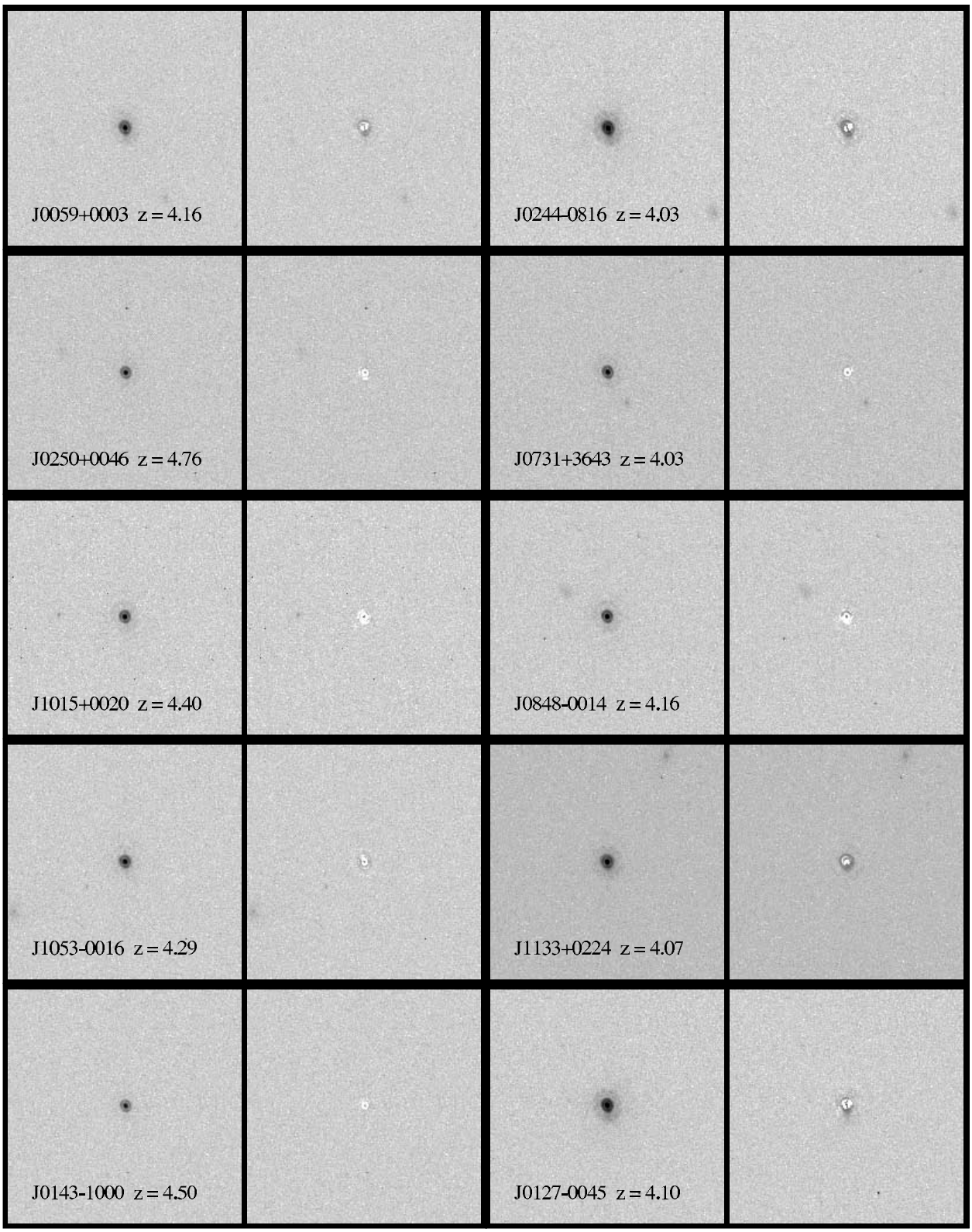

FIG. 1.—*HST* ACS HRC F775W images of the 10 high-z SDSS quasars that show any sign of a secondary object in a 5″ field of view. The scale is 5″ × 5″ in each of the panels. For each pair of images, the left panel is the CRJ output of CALACS, and the right panel is the same CRJ image after subtraction of the Tiny Tim PSF with the same stretch as the left panel.

3. CONSTRAINING THE SLOPE OF THE QUASAR LUMINOSITY FUNCTION

As discussed in Paper I, existing constraints on the high-redshift QLF are limited by sample size and to the most luminous objects. Schmidt et al. (1995), using a set of 90 quasars with $2.7 < z < 4.8$, found a power-law luminosity function slope (β) of roughly -2. Fan et al. (2001b) measured $\beta \approx -2.5 \pm 0.3$ from 39 quasars in the redshift interval 3.6–5.0. However, this relatively shallow apparent slope does not necessarily represent the intrinsic slope of the QLF, which is expected to be much steeper if a substantial fraction of these quasars are magnified by lensing (e.g., Schneider et al. 1992).

In line with Paper I and previous work, we describe the intrinsic (not necessarily observed) QLF as a broken power law (e.g., Boyle et al. 1988; Pei 1995):

$$\Phi_{\rm int}(L) = \frac{\Phi_*/L_*}{(L/L_*)^{-\beta_l} + (L/L_*)^{-\beta_h}}. \quad (1)$$

The QLF is described by four parameters: the normalization Φ_*, the faint-end slope β_l, the bright-end slope β_h, and the characteristic luminosity L_* at which the QLF steepens. The lensing probability is most sensitive to the last two parameters, β_h and L_*. The faint-end slope has negligible impact on our analysis, and we set it to $\beta_l = -1.64$ (e.g., Pei 1995). We apply the lensing model from Comerford et al. (2002), in which lenses are associated with dark matter halos, to compute the total lensing probability, including the effect of magnification bias. In this model the abundance of halos as a function of potential well depth is adopted from the simulations of Jenkins et al. (2001). As discussed in Paper I, we assume that all halos below $M \approx 10^{13}\ M_\odot$ have SIS profiles (adopting a standard conversion between circular velocity and halo mass), while all halos above this mass follow the dark matter density profile suggested by Navarro et al. (1997, hereafter NFW). NFW profiles are much less efficient lenses than are SIS profiles. This prescription is essentially equivalent to ignoring all lenses above a halo mass of $10^{13}\ M_\odot$, as the massive halos do not contribute to lensing at small separations. We do not include here more complex lens models, such as those including external shear or ellipticity. As discussed by Keeton et al. (2005), such models can, in general, boost the lensing probabilities (although that paper considered in detail only the boost that can occur for singly imaged lensing probabilities).

In the case of $\beta_h = -3.8$ and $M^*_{1450} = -24.52$, the mean probability for lensing is about 4% for each source. The morphology selection effect causes this mean probability to be reduced by about a factor of 3 (as discussed above). In Table 1 we list each of the quasars that were observed by *HST* and their lensing probabilities, which vary relatively little from source to source. The median redshift of the sample is $z = 4.35$.

The lack of lenses among these 157 quasars allows us to place constraints on the QLF at high redshift, shown in Figure 2. The lensing probability is a function of both the break and the faint-end slope. Assuming a break of $M^*_B = -25.0$ ($M^*_{1450} = -24.52$), the above lensing probabilities yield a 3 σ constraint on the bright-end slope of $\beta > -3.8$.[12] Note that we have used a somewhat brighter break luminosity than we did in Paper I for the $z \sim 6$ quasars, as the characteristic luminosity is thought to evolve with redshift. Since this choice of break luminosity is somewhat arbitrary (as it is an extrapolation from low redshift and the QLF may not even exhibit a strong break at high-z), we also show the constraints on β as a function of break luminosity in Figure 2.

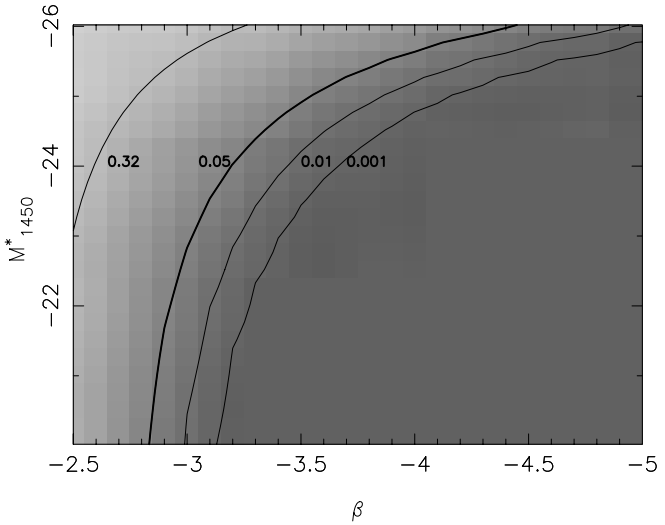

FIG. 2.—Contours of fixed likelihood for no lensing among the 157 $z \sim 4.35$ quasars, shown in the two-dimensional parameter space of the slope, and the break of the $z \sim 4.35$ QLF. The 3 σ limit on β given an assumed break in the luminosity function of $M^*_{1450} = -24.5$ is $\beta = -3.8$.

Finally, it is useful to consider constraints that we can place on the underlying lensing halo population. Without any magnification bias, the total optical depth to multiply imaged lensing at $z \sim 4.5$ is only 0.25%, which is reduced by the SDSS morphological selection to 0.08%. This makes the lack of lenses among our 157 sources unsurprising. We find that to reduce the probability of not finding even one lens in the whole sample, the single-object lensing probability must be boosted by a factor of about 40 (this is essentially the typical magnification bias produced by the model QLF we constrain at 3 σ). As a result, we rule out (at 3 σ confidence) lensing models in which there are $\gtrsim$40 times more galaxies than are implied by the halo mass function we adopted from Jenkins et al. (2001). While this is a weak constraint, it is still the best direct limit on the number density of $M \sim 10^{12}\ M_\odot$ halos at $1 < z < 2$ (the redshift and mass range dominating the expected lensing probability; see Fig. 1 in Comerford et al. 2002).

4. DISCUSSION AND CONCLUSIONS

Constraining the high-z QLF slope is particularly important to understanding the roles of accretion and feedback in the growth of galaxies (e.g., Silk & Rees 1998; Fabian 1999; Wyithe & Loeb 2003b; Hopkins et al. 2005a). For the most luminous quasars with $z \lesssim 2.5$ (i.e., the redshift at which the quasar comoving density peaks), the bright-end slope has been shown to be $\beta \sim -3.3$ (Croom et al. 2004; Richards et al. 2005). For the most luminous quasars at $z > 4$, the measured slope is $\beta \sim -2.5$ (Fan et al. 2001a). While the slope of the QLF has been well measured, understanding the physical processes behind the QLF and its evolution are still open questions, and various explanations have been proposed. Wyithe & Loeb (2003a) suggest that feedback mechanisms may prevent the gas in the most massive dark matter halos from collapsing at low-z, suppressing the number of luminous low-z quasars relative to high-z. Alternatively, in the model of Hopkins et al. (2005a, 2005b) the bright end of the QLF is defined by near-Eddington accretion at the peak luminosity in the history of a quasar, whereas the faint-end slope may be due to

[12] This constraint weakens if the intrinsic bright-end slope steepens with luminosity instead of being a single power law.

sub-Eddington accretion. Tighter limits on the bright-end slope of the high-redshift QLF provide important constraints that any such models must account for.

In this work, we have obtained high-resolution *HST* images of 157 $4 < z < 5.4$ redshift quasars (known prior to 2001 September) to look for the signature of gravitational lensing. We have found no evidence of multiple images, significantly limiting the amount by which these quasars can be magnified by foreground mass concentrations (in the absence of microlensing). The lack of any strong lenses puts a 3 σ constraint on the intrinsic bright-end slope of the $z = 4$–5 luminosity function of $\beta_h > -3.8$. Our sample has a strong bias against pairs with $\theta > 1''$ due to the exclusion of objects that appear extended in SDSS images. We are currently exploring methods for cleanly selecting such wide separation pairs from the SDSS imaging data.

Funding for the creation and distribution of the SDSS archive has been provided by the Alfred P. Sloan Foundation, the Participating Institutions, the National Aeronautics and Space Administration, the National Science Foundation, the US Department of Energy, the Japanese Monbukagakusho, and the Max Planck Society. The SDSS Web site is at http://www.sdss.org. The SDSS is managed by the ARC for the Participating Institutions. The Participating Institutions are the University of Chicago, Fermilab, the Institute for Advanced Study, the Japan Participation Group, The Johns Hopkins University, the Korean Scientist Group, Los Alamos National Laboratory, the Max Planck Institute for Astronomy (MPIA), the Max Planck Institute for Astrophysics (MPA), New Mexico State University, University of Pittsburgh, University of Portsmouth, Princeton University, the US Naval Observatory, and the University of Washington. Support for program 9472 was provided by NASA through a grant (*HST*-GO-09472.01-A; M. A. S. and G. T. R.) from the Space Telescope Science Institute, which is operated by the Association of Universities for Research in Astronomy, Inc., under NASA contract NAS5-26555. This work was supported in part by NASA ATP grant NNG 04GI88G (Z. H.) and National Science Foundation grants AST 03-07582 (D. P. S.), AST 03-07409 (M. A. S.), AST 03-07384 (X. F.), AST 03-07291 (Z. H.), and AST 03-07200 (Z. H.). X. F. and D. J. E. acknowledge Alfred P. Sloan Research Fellowships. X. F. further acknowledges support from a David and Lucile Packard Fellow in Science and Engineering.

REFERENCES

Abazajian, K., et al. 2003, AJ, 126, 2081
Anderson, S. F., et al. 2001, AJ, 122, 503
Boyle, B. J., Shanks, T., & Peterson, B. A. 1988, MNRAS, 235, 935
Browne, I. W. A., et al. 2003, MNRAS, 341, 13
Cen, R., & Haiman, Z. 2000, ApJ, 542, L75
Comerford, J. M., Haiman, Z., & Schaye, J. 2002, ApJ, 580, 63
Croom, S. M., Smith, R. J., Boyle, B. J., Shanks, T., Miller, L., Outram, P. J., & Loaring, N. S. 2004, MNRAS, 349, 1397
Eisenstein, D. J., & Hu, W. 1999, ApJ, 511, 5
Fabian, A. C. 1999, MNRAS, 308, L39
Fan, X., Narayanan, V. K., Strauss, M. A., White, R. L., Becker, R. H., Pentericci, L., & Rix, H. 2002, AJ, 123, 1247
Fan, X., et al. 1999, AJ, 118, 1
———. 2000, AJ, 119, 1
———. 2001a, AJ, 121, 31
———. 2001b, AJ, 121, 54
———. 2003, AJ, 125, 1649
Haiman, Z., & Loeb, A. 2001, ApJ, 552, 459
Hinshaw, G., & Krauss, L. M. 1987, ApJ, 320, 468
Hopkins, P. F., Hernquist, L., Cox, T. J., Di Matteo, T., Robertson, B., & Springel, V. 2005a, ApJ, 630, 716
———. 2005b, ApJ, 632, 81
Jenkins, A., Frenk, C. S., White, S. D. M., Colberg, J. M., Cole, S., Evrard, A. E., Couchman, H. M. P., & Yoshida, N. 2001, MNRAS, 321, 372
Keeton, C. R., Kuhlen, M., & Haiman, Z. 2005, ApJ, 621, 559
Krist, J. 1995, in ASP Conf. Ser. 77, Astronomical Data Analysis Software and Systems IV, ed. R. A. Shaw, H. E. Payne, & J. J. E. Hayes (San Francisco: ASP), 349
Madau, P., Haardt, F., & Rees, M. J. 1999, ApJ, 514, 648
Mesinger, A., & Haiman, Z. 2004, ApJ, 611, L69
Narayan, R. 1989, ApJ, 339, L53
Navarro, J. F., Frenk, C. S., & White, S. D. M. 1997, ApJ, 490, 493 (NFW)
Pei, Y. C. 1995, ApJ, 438, 623
Pindor, B., Turner, E. L., Lupton, R. H., & Brinkmann, J. 2003, AJ, 125, 2325
Richards, G. T., et al. 2002, AJ, 123, 2945
———. 2004, AJ, 127, 1305 (Paper I)
———. 2005, MNRAS, 360, 839
Schmidt, M., Schneider, D. P., & Gunn, J. E. 1995, AJ, 110, 68
Schneider, D. P., et al. 2001, AJ, 121, 1232
———. 2005, AJ, 130, 367
Schneider, P., Ehlers, J., & Falco, E. E. 1992, Gravitational Lenses (Berlin: Springer)
Silk, J., & Rees, M. J. 1998, A&A, 331, L1
Spergel, D. N., et al. 2003, ApJS, 148, 175
Turner, E. L. 1991, AJ, 101, 5
Turner, E. L., Ostriker, J. P., & Gott, J. R. 1984, ApJ, 284, 1
Wyithe, J. S. B. 2004, MNRAS, 351, 1266
Wyithe, J. S. B., & Loeb, A. 2002, ApJ, 577, 57
———. 2003a, ApJ, 586, 693
———. 2003b, ApJ, 595, 614
———. 2004, Nature, 432, 194
York, D. G., et al. 2000, AJ, 120, 1579
Zheng, W., et al. 2000, AJ, 120, 1607